RELATIONS AMONG pH, SULFATE, AND METALS CONCENTRATIONS IN ANTHRACITE AND BITUMINOUS COAL-MINE DISCHARGES, PENNSYLVANIA[1]

Charles A. Cravotta III [2]

Abstract. Water-quality data for discharges from 140 abandoned mines in the Bituminous and Anthracite Coalfields of Pennsylvania illustrate relations among pH, sulfate, and dissolved metal concentrations. The pH for the 140 samples ranged from 2.7 to 7.3, with two modes at pH 2.5 to 4 (acidic) and 6 to 7 (near neutral). Generally, flow rates were smaller and solute concentrations were greater for low-pH samples; flow rates increased with pH. Although the pH distribution was similar for the bituminous and anthracite subsets, the bituminous discharges had smaller median flow rates, greater concentrations of sulfate, iron, and aluminum, and smaller concentrations of barium and lead than anthracite discharges with the same pH values. The observed relations between the pH and constituent concentrations can be attributed to (1) dilution of acidic water by alkaline ground water; (2) solubility control of aluminum, iron, manganese, barium, and lead by hydroxide, sulfate, and/or carbonate minerals; and (3) aqueous sulfate-complex formation. The formation of $AlSO_4^+$ and $AlHSO_4^{+2}$ complexes adds to the total dissolved aluminum concentration at pH of equilibrium with aluminum hydroxide or hydroxysulfate minerals and can account for 10 to 20 times greater concentrations of dissolved aluminum in bituminous discharges compared to anthracite discharges at similar pH. Sulfate complexation also can account for 10 to 30 times greater concentrations of dissolved ferric iron concentrations at equilibrium with ferrihydrite ($Fe(OH)_3$) and/or schwertmannite ($Fe_8O_8(OH)_{4.5}(SO_4)_{1.75}$) at pH of 3 to 5. In contrast, lower barium and lead concentrations in bituminous than anthracite discharges indicates elevated sulfate concentration could decrease mobility of these metals by the formation of insoluble minerals such as barite ($BaSO_4$) or anglesite ($PbSO_4$). Most samples were saturated with barite, but none were saturated with anglesite. Hence, lead concentrations could be controlled by coprecipitation with barite and/or by adsorption to schwertmannite or another sulfate-bearing oxide.

Additional Key Words: speciation, solubility, iron, aluminum, manganese, barium, lead.

---

[1] Paper presented at the 7th International Conference on Acid Rock Drainage (ICARD), March 26-30, 2006, St. Louis MO. R.I. Barnhisel (ed.) Published by the American Society of Mining and Reclamation (ASMR), 3134 Montavesta Road, Lexington, KY 40502

[2] Charles A. Cravotta III is Research Hydrologist, U.S. Geological Survey, New Cumberland, PA 17070.

7th International Conference on Acid Rock Drainage, 2006 pp 378-404
DOI: 10.21000/JASMR06020378

http://dx.doi.org/10.21000/JASMR06020378

Introduction

Abandoned mine drainage (AMD) can be corrosive or encrusting and can foul aquatic habitat, water-delivery systems, bridges, and associated infrastructure (Barnes and Clarke, 1969; Winland et al., 1991; Bigham and Nordstrom, 2000; Houben, 2003). Although dissolved SO_4^{-2}, Fe, Al, and Mn are widely recognized as mineral constituents of concern, numerous trace metals also have been documented in AMD, particularly in strongly acidic, low-pH solutions (Hyman and Watzlaf, 1997; Rose and Cravotta, 1998; Nordstrom and Alpers, 1999; Nordstrom, 2000; Nordstrom et al., 2000). The dissolved metals and associated constituents in AMD can be toxic to aquatic and terrestrial organisms (Smith and Huyck, 1999). Generally, the toxicity of a dissolved element increases with its concentration after nutritional requirements, if any, are met (Smith and Huyck, 1999).

The pH of a solution is an important measure for evaluating aquatic toxicity and corrosiveness. The severity of toxicity or corrosion tends to be greater under low-pH or high-pH conditions than at near-neutral pH, because the solubility of many metals can be described as amphoteric, with a greater tendency to dissolve and form cations at low pH or anions at high pH (Langmuir, 1997, p. 152). For example, $Al(OH)_3$ and aluminosilicate minerals have their minimum solubility at pH 6 to 7 (Nordstrom and Ball, 1986; Bigham and Nordstrom, 2000), and brief exposure to relatively low concentrations of dissolved Al can be toxic to fish and other aquatic organisms (Baker and Schofield, 1982; Elder, 1988). Accordingly, the U.S. Environmental Protection Agency (2000, 2002a, 2002b) recommends pH 6.5 to 9.0 for protection of freshwater aquatic life and pH 6.5 to 8.5 for public drinking supplies. Nevertheless, pH is not the sole determinant of metals solubility.

Anions including SO_4^{-2}, HCO_3^-, and, less commonly, Cl^- can be elevated above background concentrations in AMD, and polyvalent cations such as Al and Fe tend to associate with such ions of opposite charge. Ion-pair formation or aqueous complexation reactions between dissolved cations and anions can increase the total concentration of metals in a solution at equilibrium with a mineral (e.g. Rose et al., 1979; Ball and Nordstrom, 1991; Langmuir, 1997; Nordstrom, 2004). Hence, aqueous complexation or speciation is likely to affect the concentration or transport of metals in AMD.

This report examines relations between the pH, SO_4^{-2}, and metals concentrations in a variety of AMD samples collected from the Bituminous and Anthracite Coalfields in Pennsylvania in 1999. Similarities and differences between the data for flow rate and chemistry as a function of pH for the anthracite and bituminous AMD samples are explored. The potential formation of aqueous species and stability of possible solid phases in contact with samples are evaluated with respect to thermodynamic equilibrium at near-surface temperature and pressure conditions.

Study Area and Methods

Description of Study Area

Bituminous coal deposits underlie western and north-central Pennsylvania, and anthracite deposits underlie east-central and northeastern Pennsylvania (Fig. 1). The mineable coals are interbedded with shale, siltstone, sandstone, conglomerate, and occasional limestone (Berg et al., 1989; Brady et al., 1998). Pennsylvania's Bituminous Coalfield lies within the Appalachian Plateaus Physiographic Province and is characterized by gently dipping strata; nearly horizontal

coalbeds commonly crop out in the incised stream valleys (Berg et al., 1989; Edmunds, 1999). Pennsylvania's Anthracite Coalfield lies within the Ridge and Valley Physiographic Province and is characterized by complexly deformed strata; mineable coalbeds typically extend beneath valleys in steeply folded and fractured synclinal troughs (Wood et al., 1986; Eggleston et al., 1999).

During the past 200 years, the coal deposits in Pennsylvania have been extensively mined as sources of industrial and domestic fuel (Northern and Central Appalachian Basin Coal Regions Assessment Team, 2000). The historical mining was conducted with little regard for the environment; upon closure, mine voids were left open and surrounding landscapes were covered with unrelaimed spoil. Storm runoff from widely distributed, unreclaimed spoil banks and discharges from abandoned, flooded mines contributed sediment, H_2SO_4, and metals to streams in mined areas. Consequently, historical coal mines degrade more than 5,000 kilometers of streams in Pennsylvania (Pennsylvania Department of Environmental Protection, 2002).

Sample Site Selection

In summer and fall 1999, discharges from 140 abandoned coal mines in the Anthracite and Bituminous Coalfields of Pennsylvania (Fig. 1) were sampled for analysis of chemical concentrations and loading. The 140 discharges were selected among thousands of AMD sources statewide based on their geographic distribution, accessibility, and potential for substantial loadings of dissolved metals. Most of the sampled discharges were from underground mines. The 41 anthracite discharges previously had been studied by the U.S. Geological Survey (USGS) (Growitz et al., 1985; Wood, 1996). The 99 bituminous discharges previously had been studied by the Southern Alleghenies Conservancy (1998).

Water-Quality Sampling and Analysis

Field data for flow rate, temperature, specific conductance (SC), dissolved oxygen (DO), pH, and redox potential (Eh) were measured at each site when samples were collected in accordance with standard methods (Rantz et al., 1982a, 1982b; Wood, 1976; U.S. Geological Survey, variously dated; Ficklin and Mosier, 1999). All meters were calibrated in the field using electrodes and standards that had been thermally equilibrated to sample temperatures. Field pH and Eh were determined using a combination Pt and Ag/AgCl electrode with a pH sensor. The electrode was calibrated in pH 2.0, 4.0, and 7.0 buffer solutions and in ZoBell's solution (Wood, 1976; U.S. Geological Survey, variously dated). Values for Eh were corrected to 25 °C relative to the standard hydrogen electrode in accordance with methods of Nordstrom (1977).

To minimize effects from aeration, electrodes were immersed and samples were collected as close as possible to the point of discharge. Water samples were collected into 3-L Teflon bottles and then split into sample-rinsed polyethylene bottles. An unfiltered subsample for analysis of acidity and alkalinity was capped leaving no head space and stored on ice. Two subsamples for analysis of "dissolved" anions and cations plus silica were filtered through a 0.45-μm pore-size nitrocellulose capsule filter. The subsample for cation analysis was preserved with trace-element grade nitric acid to $pH < 2$.

All samples were processed using standard methods for analysis of alkalinity, acidity, anions, and cations. The fresh, unfiltered subsamples were analyzed for alkalinity in the laboratory within 48 hours of sampling by titration with H_2SO_4 to the endpoint pH of 4.5 (American Public Health Association, 1998b). The acidity was determined on aged, oxidized samples by titration

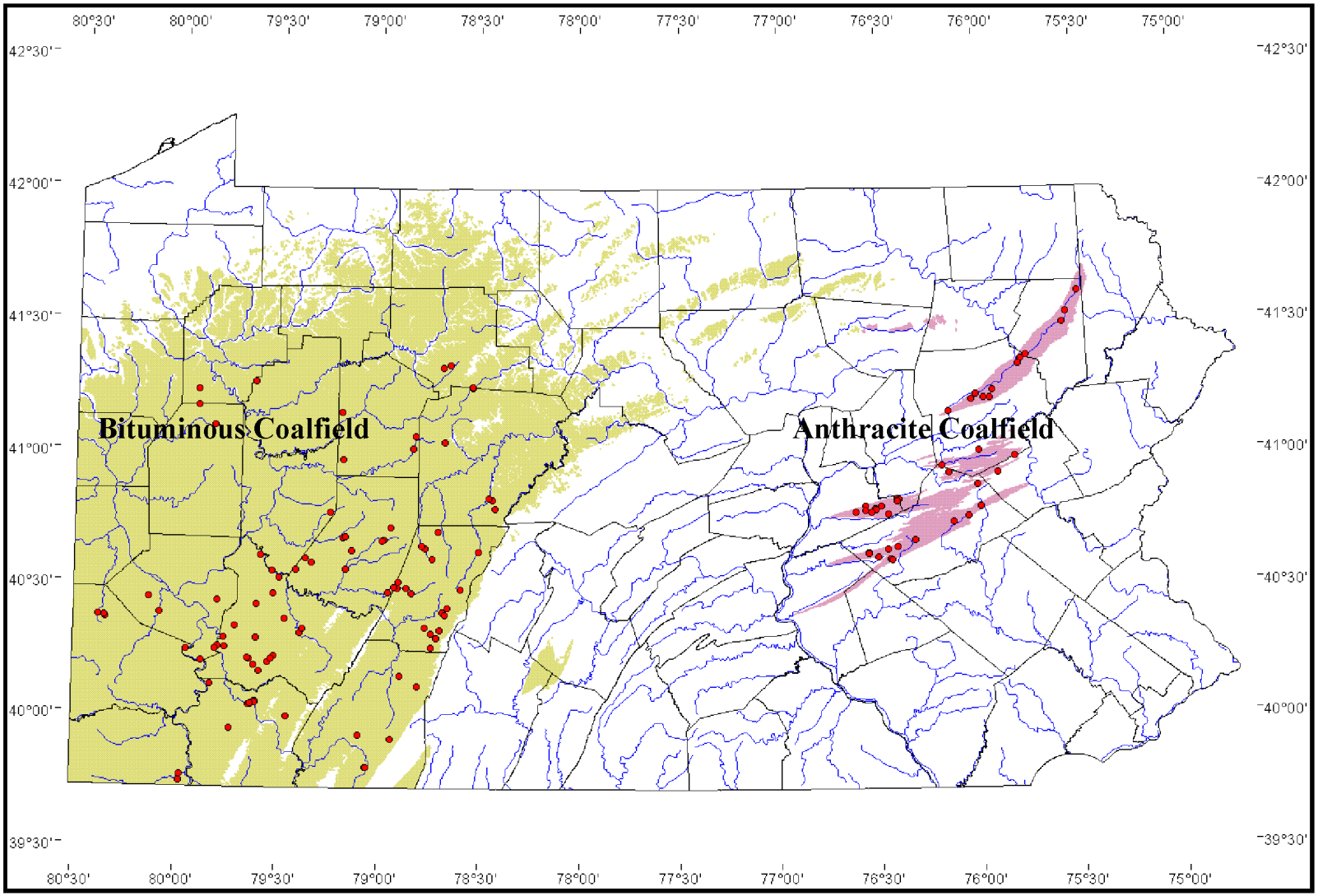

Figure 1. Map of Pennsylvania showing locations of 140 abandoned mine discharge sites in the Anthracite and Bituminous Coalfields that were sampled in 1999 by the USGS (Cravotta and Kirby, 2004). Coalfield boundaries based on distribution of Pennsylvanian Age bedrock (Berg et al., 1980).

with NaOH to the endpoint pH of 8.3, after the addition of H_2SO_4 and H_2O_2, boiling, and cooling (American Public Health Association, 1998a; Cravotta and Kirby, 2004). The pH before and during titrations was measured using a liquid-filled combination Ag/AgCl pH electrode calibrated in pH 4.0, 7.0, and 10.0 buffer solutions. Sulfate, Cl^-, F^-, nitrate, nitrite, and phosphate in the filtered, unpreserved samples were analyzed by ion chromatography (IC) (Fishman and Friedman, 1989; Crock et al., 1999). Concentrations of major cations, silica, and trace elements in the filtered, acidified samples were determined using inductively coupled plasma atomic emission spectroscopy (ICP-AES) and inductively coupled plasma emission mass spectrometry (ICP-MS) (Fishman and Friedman, 1989; Crock et al., 1999). All samples were analyzed in replicate by one or more of the methods and at two or more laboratories. Results for replicate analyses were averaged before evaluation. Charge imbalances routinely were less than 5% relative to the mean of cation and anion equivalents.

Computation of Acidity

The net acidity was computed considering positive contributions from pH and dissolved Fe, Mn, and Al concentrations (C_{Fe}, C_{Mn}, C_{Al}, respectively), in milligrams per liter, and negative contributions from alkalinity as:

$$\text{Acidity}_{\text{computed}}\ (\text{mg L}^{-1}\ \text{CaCO}_3) = 50\cdot(10^{(3\text{-pH})} + 2\cdot C_{Fe}/55.85 + 2\cdot C_{Mn}/54.94 + 3\cdot C_{Al}/26.98) - \text{Alkalinity}\ (\text{mg L}^{-1}\ \text{CaCO}_3). \quad (1)$$

Cravotta and Kirby (2004) and Kirby and Cravotta (2005a, b) demonstrated with data for samples evaluated in this paper that acidity computed with Equation (1) is comparable in value to the standard method "hot peroxide" acidity where the H_2SO_4 added to the sample is subtracted from the NaOH added (American Public Health Association, 1998a).

Aqueous Speciation Computations

Activities of aqueous species, partial pressure of carbon dioxide (Pco_2), and mineral-saturation index (SI) values were calculated using the WATEQ4F version 2.63 computer program (Ball and Nordstrom, 1991). The Pco_2 was computed on the basis of measured pH, alkalinity, and temperature. The concentrations and activities of Fe^{+2} and Fe^{+3} species were computed on the basis of the measured dissolved Fe, Eh, and temperature of fresh samples. Nordstrom (1977) and Nordstrom et al. (1979) have shown there is good agreement between the measured Eh and that predicted by the Fe^{+2}/ Fe^{+3} couple in acidic mine waters.

Spreadsheet models were developed to evaluate the theoretical levels of specific elements (Al, Fe, Mn, Ca, Ba, Pb, Zn) at equilibrium with OH^-, SO_4^{-2}, and CO_3^{-2} minerals (solubility) and the associated activities of aqueous species of that element as a function of the pH, Pco_2, and concentration of SO_4^{-2} and Cl^-. The theoretical solubilities and activities were computed and plotted as reference lines on "pC-pH diagrams." Then, the measured concentration of the element and, in some cases, activities of uncomplexed cations (Al^{+3}, Fe^{+3}, Fe^{+2}) computed with WATEQ4F were plotted relative to the measured pH on the same diagram. Reactions and associated equilibrium constants for relevant species and solids were obtained mostly from the WATEQ4F thermodynamic database (Ball and Nordstrom, 1991; Drever, 1997) and supplemented with data for Fe^{+3} minerals from other sources (Bigham et al., 1996; Yu et al., 1999). Speciation and solubility reactions and values for equilibrium constants that were used are summarized in the appendix Tables A1-A3. For example, Pb^{+2} equilibrium reactions and constants are given in detail in Table A3, because thermodynamic data were available for the corresponding OH^-, SO_4^{-2}, and CO_3^{-2} minerals and aqueous species. Only a subset of aqueous

speciation reactions were considered for the spreadsheet computations, and the measured concentration of the dissolved element rather than activity was plotted relative to activity boundaries.

Relations among pH, Sulfate, and Dissolved Metals in Mine Drainage

Characteristics of Anthracite and Bituminous AMD Samples

Data on the flow rates, pH, acidity, alkalinity, and selected solute concentrations for the 140 AMD samples collected in 1999 from abandoned coal mines in the Anthracite and Bituminous Coalfields of Pennsylvania are summarized in Table 1 and Fig. 2. Sampled flow rates at the 140 AMD sites ranged from 0.028 to 2,210 L sec^{-1}. The anthracite discharges had greater median flow rates than the bituminous discharges (Table 1). Furthermore, median and maximum flow rates for the anthracite mine discharges generally exceeded those for the bituminous mines for the same pH class interval (Fig. 2)

Median flow rates for bituminous and anthracite discharges increased with pH, implying that neutralization of AMD did not result solely by mineral dissolution but also involved dilution of initially acidic water by alkaline ground water or surface water, hence increasing both the volume and pH. Generally, alkalinity increased and concentrations of other major solutes decreased with increased pH (Fig. 2), consistent with dilution. Larger flow rates for anthracite discharges than bituminous discharges reflect differences in the physiographic and geologic settings between the two coalfields (Berg et al., 1989; Edmunds, 1999; Eggleston et al., 1999) and indicate that, on average, the anthracite mines have larger recharge areas and more extensive flooded volumes compared to the bituminous mines. Because anthracite mine complexes historically connected multiple coalbeds and extended beneath valleys to hundreds of meters below the regional water table, their mined areas and associated discharge volumes tend to be substantially greater than those from contemporaneous surface mines or bituminous mines that access one or two coalbeds within isolated hilltops.

The pH of the 140 fresh AMD samples ranged from 2.7 to 7.3, with the majority either acidic (pH 2.5 to 4) or near neutral (pH 6 to 7) (Table 1, Fig. 2). This bimodal frequency distribution of pH for the AMD samples was discussed in detail by Cravotta et al. (1999) and Cravotta and Kirby (2004). Although the minimum and maximum pH values were associated with bituminous mine discharges, the median pH values of 5.1 and 5.2 were similar for the 41 anthracite and 99 bituminous discharges, respectively (Table 1). Dissolved aluminum, zinc, and lead concentrations and, to a lesser extent, SO_4^{-2} and Mn concentrations, were inversely correlated with pH; iron concentrations were not correlated with pH; and barium and alkalinity concentrations were positively correlated with pH (Fig. 2).

Alkalinity concentrations ranged from 0 (pH < 4.4; 50 samples) to 510 mg L^{-1} as $CaCO_3$ (Table 1). For the 90 samples that had alkalinity > 0, the computed Pco_2 values by WATEQ4F ranged from $10^{-2.45}$ to $10^{-0.54}$ atm, which are 10 to 1,000 times greater than atmospheric Pco_2 of $10^{-3.5}$ atm. The median Pco_2 was $10^{-1.0}$ atm ($-\log(Pco_2, atm) = pCO_2 = -1.0$). Computed acidity concentrations, which exclude contributions from dissolved CO_2, ranged from -326 to 1,587 mg L^{-1} as $CaCO_3$ (Table 1). Concentrations of dissolved SO_4^{-2}, Fe, Al, and Mn ranged from 34 to 2,000 mg L^{-1}, 0.046 to 512 mg L^{-1}, 0.007 to 108 mg L^{-1}, and 0.019 to 74 mg L^{-1}, respectively (Table 1). Generally, the highest concentrations of acidity, SO_4^{-2}, Fe, Al, Mn, and

.

Table 1. Hydrochemical characteristics of discharges from 140 abandoned coal mines in Pennsylvania, 1999[a]

[median (minimum; maximum); L sec^{-1}, liters per second; mg L^{-1}, milligrams per liter; µg L^{-1}, micrograms per liter]

Coalfield & number of samples	Flow Rate	pH, field	Alkalinity	Net Acidity, computed[b]	Oxygen; O_2	Sulfate; SO_4	Iron; Fe	Manganese: Mn	Aluminum; Al
	L sec^{-1}		mg L^{-1} as $CaCO_3$		mg L^{-1}	mg L^{-1}	mg L^{-1}	mg L^{-1}	mg L^{-1}
Anthracite N=41	64.0 (0.028; 2,210)	5.1 (3.0; 6.3)	3 (0; 120)	43 (-79; 588)	1.9 (0.3;11.1)	260 (34; 1,300)	15 (0.046; 312)	2.9 (0.019; 19)	0.280 (0.007; 26)
Bituminous N=99	12.5 (0.227; 278)	5.2 (2.7; 7.3)	14 (0; 510)	76 (-326; 1,587)	0.6 (0.2; 11.5)	580 (120; 2,000)	43 (0.16; 512)	2.3 (0.12; 74)	1.5 (0.008; 108)

Coalfield & number of samples	Arsenic; As	Barium; Ba	Boron; B	Cobalt; Co	Lead; Pb	Nickel; Ni	Selenium; Se	Yttrium; Y	Zinc; Zn
	µg L^{-1}	µg L^{-1}	µg L^{-1}	µg L^{-1}	µg L^{-1}	µg L^{-1}	µg L^{-1}	µg L^{-1}	µg L^{-1}
Anthracite N=41	0.62 (<0.03; 15)	18 (13; 31)	16 (<1; 69)	59 (0.43; 770)	0.68 (<0.1; 11)	83 (19; 620)	0.4 (<0.2; 3.9)	2.9 (0.18; 44)	130 (3.0; 1,000)
Bituminous N=99	2.0 (0.1; 64)	13 (2.0; 39)	62 (19; 260)	52 (0.27; 3,100)	0.10 (<0.1; 4.6)	90 (2.6; 3,200)	0.6 (<0.2; 7.6)	15 (0.11; 530)	140 (0.6; 10,000)

a. Sample site locations shown in Figure 1. Data are available from the U.S. Geological Survey by contacting the author.

b. Net acidity computed on the basis of the pH and dissolved aluminum, iron, and manganese concentrations (C_{Al}, C_{Fe}, and C_{Mn}, respectively), in milligrams per liter, as: $\text{Net acidity}_{computed}$ (mg L^{-1} $CaCO_3$) = $50 \cdot (10^{(3-pH)} + 3 \cdot C_{Al}/26.98 + 2 \cdot C_{Fe}/55.85 + 2 \cdot C_{Mn}/54.94)$ - Alkalinity.

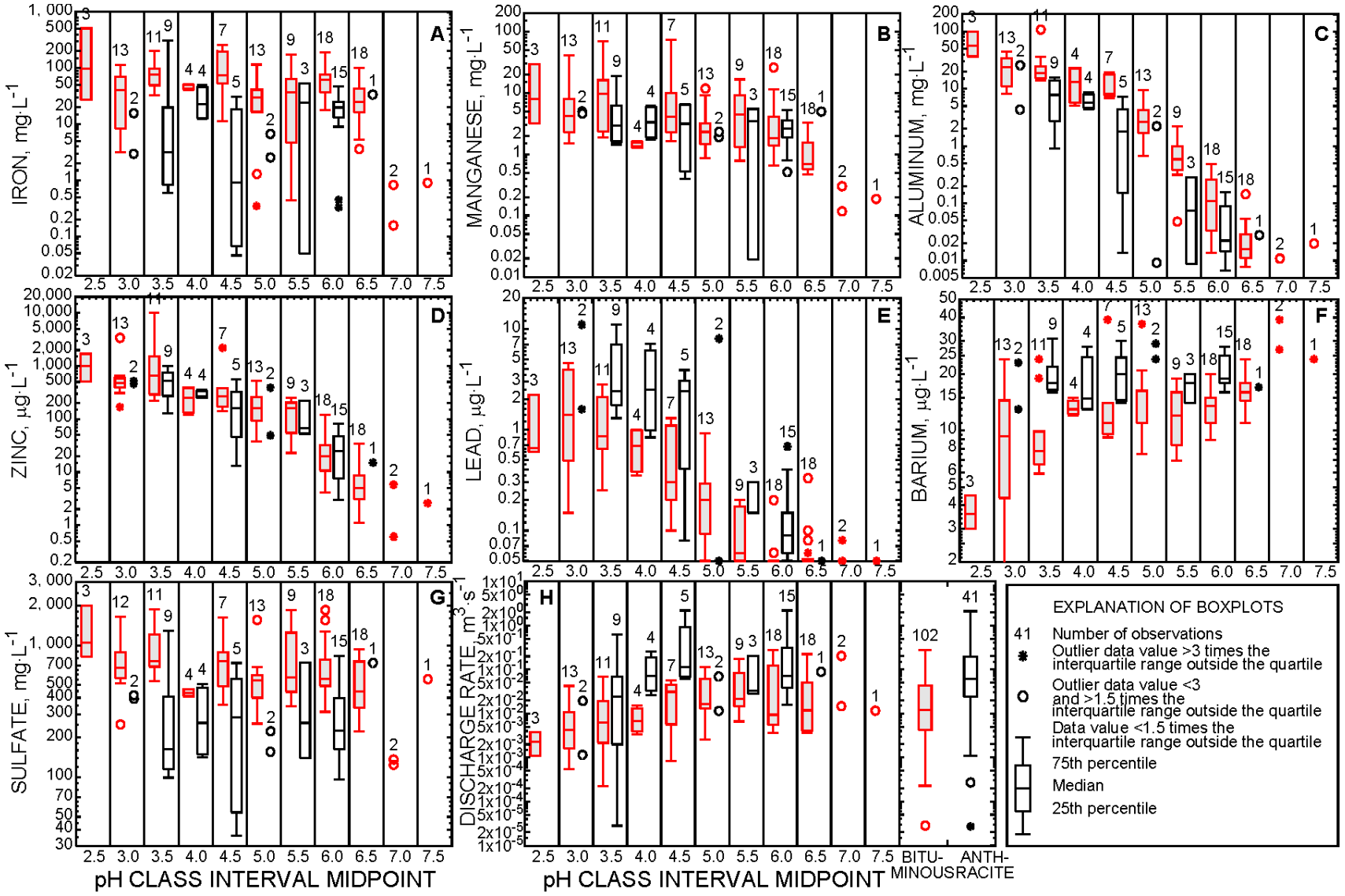

Figure 2. Boxplots showing solute concentrations and flow rate as a function of pH of 140 abandoned mine discharges in Pennsylvania, 1999: *A*, iron; *B*, manganese; *C*, aluminum; *D*, zinc; *E*, lead; *F*, barium; *G*, sulfate; *H*, flow rate. Bituminous, red; anthracite, black.

most other metals were associated with low-pH samples. Median concentrations of dissolved O_2 generally were low (<2 mg L^{-1}) throughout the range of pH, consistent with the predominance of dissolved Fe^{+2} and Mn^{+2} species in most samples.

The bituminous discharges generally contained greater concentrations of dissolved mineral constituents than the anthracite discharges as a whole (Table 1) or with the same pH values (Fig. 2) as indicated by greater median and maximum values for specific conductance and concentrations of alkalinity, acidity, SO_4^{-2}, Fe, Al, Mn, and other solutes, including As, B, Co, Ni, Se, Y, and Zn. In contrast, the median concentrations of dissolved Ba and Pb in bituminous discharges were less than those for the anthracite discharges (Table 1, Fig. 2). As noted above, relatively low concentrations of dissolved mineral constituents in the anthracite discharges could result from dilution of initially acidic AMD with a fresh-water source containing few dissolved solids. Such dilution could affect aqueous speciation and mineral solubilities.

Aqueous Speciation and Mineral Solubility Controls of Constituents in AMD Samples

Dissolved Al and SO_4^{-2} concentrations typically were elevated for the low-pH (< 5), acidic AMD samples, mainly from bituminous mines (Fig. 2). Computed SI values indicated samples with pH < 4 were undersaturated with respect to most Al minerals (Figs. 3D-3F), including amorphous $Al(OH)_3$, gibbsite ($Al(OH)_3$), basaluminite ($Al_4(OH)_{10}(SO_4)$), alunite ($KAl_3(SO_4)_2(OH)_6$), allophane ($[Al(OH)_3]_{(1-x)}[SiO_2]_{(x)}$ where x = 1.24-0.135 pH), kaolinite ($Al_2Si_2O_5(OH)_4$), illite ($K_{0.6}Mg_{0.25}Al_{2.3}Si_{3.5}O_{10}(OH)_2$), chlorite ($Mg_5Al_2Si_3O_{10}(OH)_8$), and other aluminosilicates. Hence, kaolinite, illite, and chlorite in shale associated with anthracite and bituminous coal deposits (e.g. Cravotta, 1994; Cravotta et al., 1994) could be sources of dissolved Al in the low-pH samples.

Equilibrium computations indicated concentrations of Al and activities of Al^{+3} for the AMD samples could be limited at pH $\geq$ 5.5 by the precipitation of amorphous to poorly crystalline $Al(OH)_3$, kaolinite, and/or allophane and at pH < 5.5 by a jurbanite-like phase ($Al(SO_4)(OH)\cdot 5H_2O$) (Figs. 3F and 4B). The solubility of jurbanite at low pH coincides with observed concentrations of total dissolved Al in the AMD samples (Fig. 4B) and its apparent supersaturation is consistent with computed SI values ranging to 1.2. Amorphous Al hydroxysulfate precipitates have been reported for a variety of AMD sites (e.g. Nordstrom and Ball, 1986; Robbins et al., 1996, 1999; Thomas and Romanek, 2002). However, according to Bigham and Nordstrom (2000), the mineral jurbanite is crystalline and its apparent saturation for acid SO_4^{-2} waters is fortuitous and not indicative of solubility equilibrium. Bigham and Nordstrom (2000) argued that if jurbanite or another phase with similar stoichiometry limited the concentration of dissolved Al in AMD, an inverse correlation between Al and SO_4^{-2} would be expected for low-pH samples instead of the observed positive correlation.

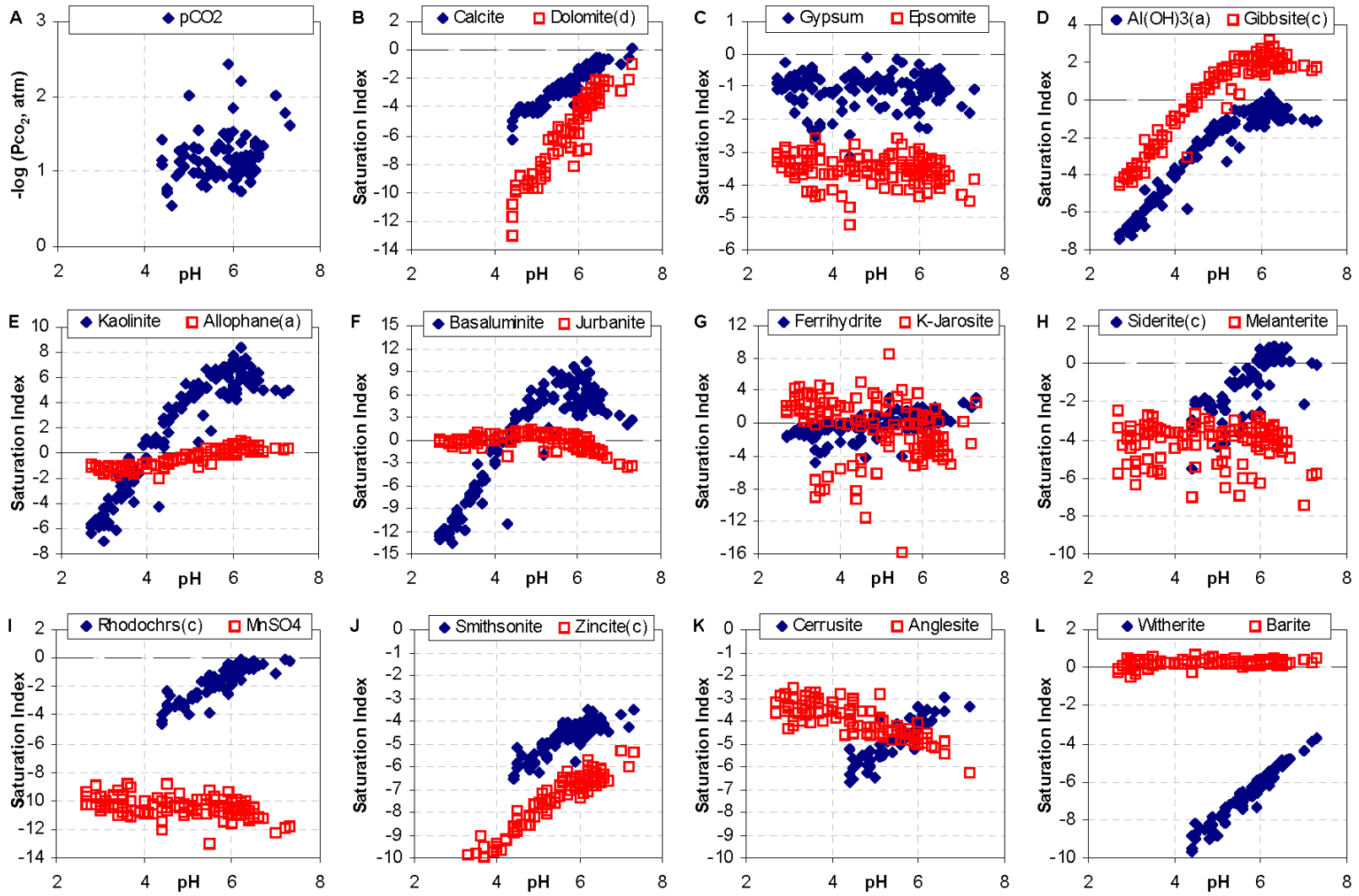

Figure 3. Partial pressure of CO_2 and saturation indices for various solids as a function of pH of 140 abandoned mine discharges in Pennsylvania, 1999, by WATEQ4F (Ball and Nordstrom, 1991). *A*, partial pressure of CO_2; *B*, calcite and dolomite; *C*, gypsum and epsomite; *D*, amorphous $Al(OH)_3$ and gibbsite; *E*, kaolinite and allophane; *F*, basaluminite and jurbanite; *G*, ferrihydrite and jarosite; *H*, siderite and melanterite; *I*, rhodochrosite and $MnSO_4$; *J*, smithsonite and zincite; *K*, cerrusite and anglesite; *L*, witherite and barite. Solids, as identified in WATEQ4F, have parenthetical letters indicating: a, amorphous; c, crystalline; d, disordered.

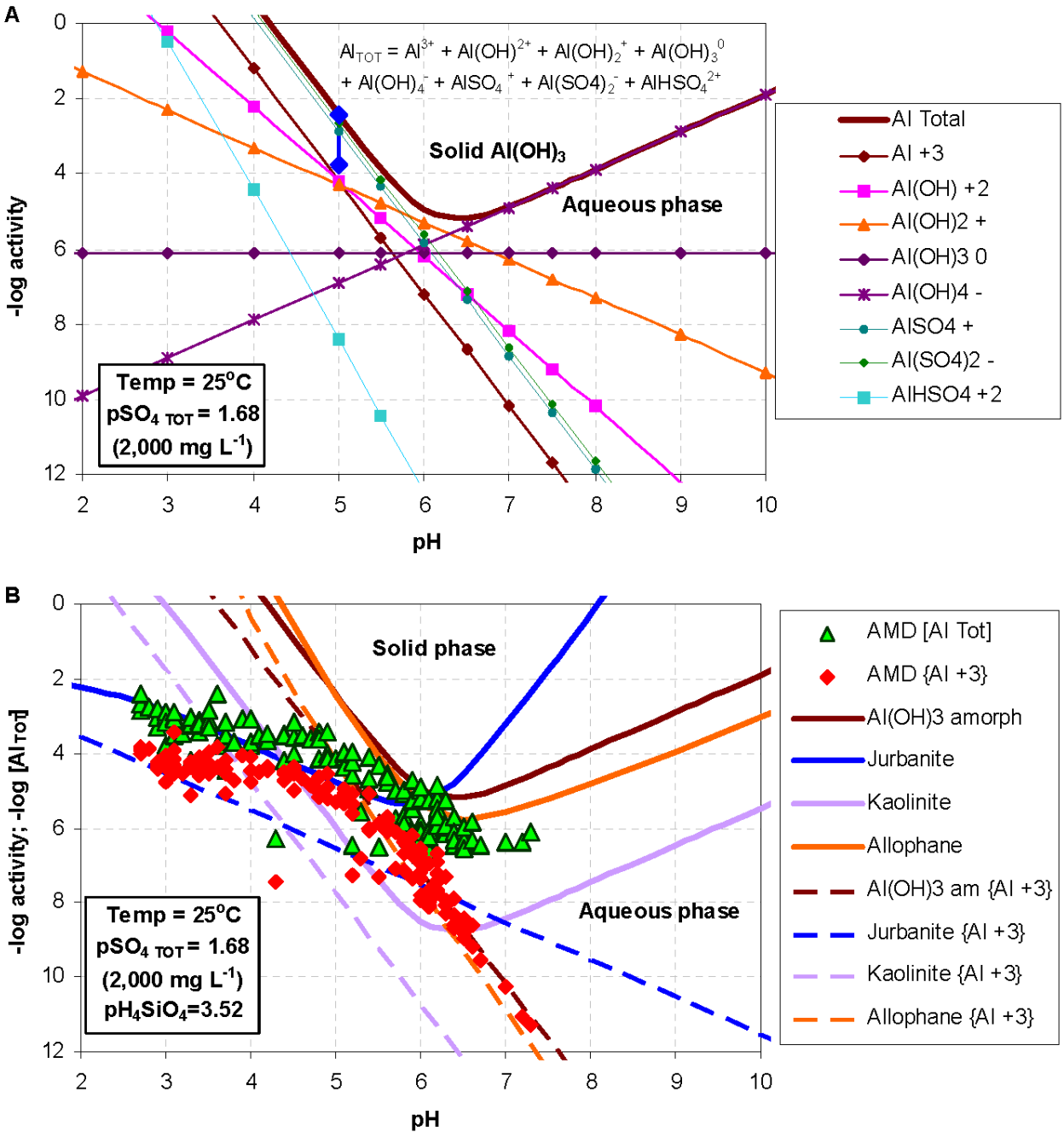

Figure 4. Aluminum solubility at 25 °C as a function of pH and sulfate concentration: *A*, Aluminum-hydroxyl and -sulfate complexes at equilibrium with amorphous aluminum hydroxide, 2,000 mg L^{-1} total sulfate; lower blue diamond indicates solubility if sulfate absent at pH = 5. *B*, Total dissolved aluminum concentration for 140 AMD samples and stability limits for amorphous $Al(OH)_3$, a "jurbanite-like" phase ($Al(SO_4)(OH)\cdot 5H_2O$), kaolinite ($Al_2Si_2O_5(OH)_4$), and allophane ($[Al(OH)_3]_{(1-x)}[SiO_2]_{(x)}$ where x = 1.24-0.135·pH). Thermodynamic data from Ball and Nordstrom (1991).

Greater concentrations of dissolved Al in bituminous discharges and the general decline in dissolved Al concentration with increased pH are consistent with aluminum-sulfate complexing and solubility control by aluminum-hydroxide and hydroxysulfate minerals (Figs. 4A and 4B). The concentration of dissolved Al at equilibrium with solid $Al(OH)_3$ will increase with increased concentration of sulfate due to formation of aluminum-sulfate complexes, particularly at pH < 5. Speciation computations demonstrated that the formation of $AlSO_4^+$ and $AlHSO_4^{+2}$ could increase the solubility, or total concentration, of Al. For example, adding 2,000 mg L^{-1} of SO_4^{-2} resulted in a 20-fold increase in the total Al concentration at equilibrium with $Al(OH)_3$ at pH 5 (Fig. 4A), consistent with greater concentrations of Al and SO_4^{-2} in bituminous than anthracite discharges (Fig. 2). In contrast, neutralization and/or dilution could result in the precipitation of Al minerals.

The pC-pH diagrams for Fe and Mn (Figs. 5 and 6) provide a basis for evaluating the stabilities of various Fe^{+3}, Fe^{+2}) and Mn^{+2} minerals over the observed ranges of pH and solute concentrations, and considering various solubilities for the minerals (e.g. Whittemore and Langmuir, 1975; Alpers et al., 1989; Bigham et al., 1996; Yu et al., 1999). As with Al, speciation computations indicated that the formation of $FeSO_4^+$ and $FeHSO_4^{+2}$ could increase the solubility, or total concentration, of Fe^{+3} (Fig. 5A), consistent with greater concentrations of Fe and SO_4^{-2} in bituminous than anthracite discharges (Fig. 2). Nevertheless, the poor correlation between pH and concentrations of total dissolved Fe and Mn (Fig. 2) implies a large fraction of these metals was present as Fe^{+2} and Mn^{+2} (Figs. 6A and 6B), which are not controlled by hydroxide-mineral solubility nor affected by SO_4^{-2} complexation under the sampled conditions ($SO_4^{-2} \leq 2{,}000$ mg L^{-1} and pH $\leq$ 7.3).

Although the majority of dissolved iron over the range of pH (2.6 - 7.3) for the AMD samples was present as Fe^{+2} species, Fe^{+3} species also were present, but at low concentrations. The computed activities of Fe^{+3} for the AMD samples were inversely correlated with pH and closely aligned with theoretical Fe^{+3} activity boundaries for hydrous Fe(III) oxides and sulfates (Fig. 5B). Generally, the corresponding pFe^{+3} and pH values for the AMD samples were at or near equilibrium with ferrihydrite ($Fe(OH)_3$) or schwertmannite ($Fe_8O_8(OH)_{4.5}(SO_4)_{1.75}$) but exceeded equilibrium values for goethite (FeOOH) and jarosite ($KFe_3(SO_4)_2(OH)_6$) (Figs. 3G and 5B).

Although variations in crystallinities and compositions of precipitated Fe(III) phases (Whittemore and Langmuir, 1975; Yu et al., 1999) can account for some discordance between the computed Fe^{+3} activity for AMD samples and the theoretical stability limits for solid phases controlling the Fe^{+3} activities at a given pH, kinetic factors also must be considered. For example, the apparent supersaturation of AMD samples with respect to goethite and jarosite (Fig. 5B) results because of kinetic barriers to the formation of these minerals and indicates the precipitation of jarosite or goethite probably could not control the Fe^{+3} activities or total Fe^{III} concentrations for the AMD samples. Goethite commonly observed at AMD sites (e.g. Winland et al., 1991; Williams et al., 2002) could form by gradual transformation from metastable schwertmannite or ferrihydrite precipitates (Miller, 1980; Bigham et al., 1996).

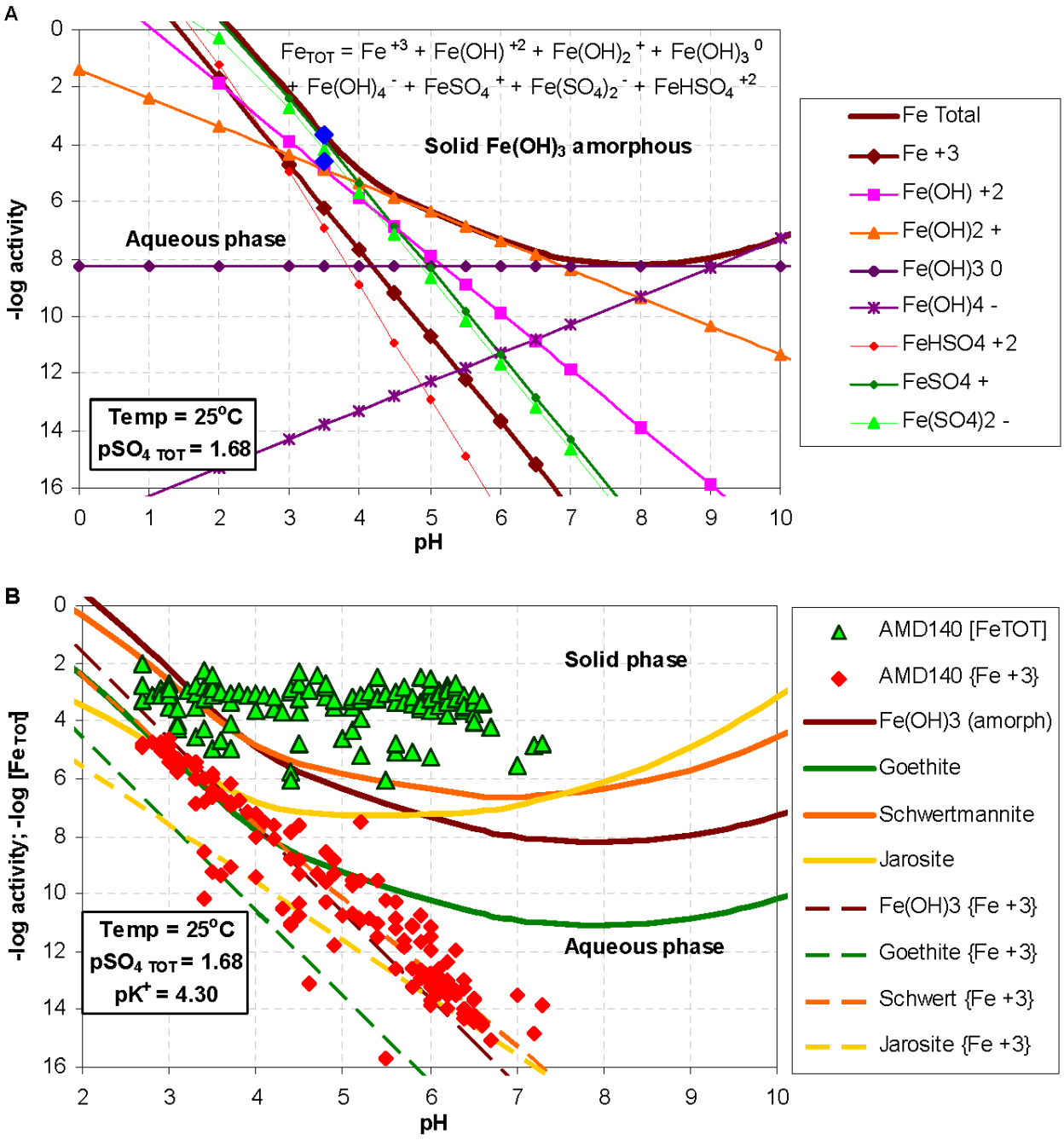

Figure 5. Ferric iron solubility at 25 °C as a function of pH and sulfate concentration: *A*, Ferric-hydroxyl complexes at equilibrium with amorphous ferric hydroxide, 2,000 mg L^{-1} total sulfate; lower blue diamond indicates solubility if sulfate absent at pH = 3. *B*, Total dissolved iron concentration and ferric ion activity for 140 AMD samples and potential solubility control by amorphous $Fe(OH)_3$, goethite (FeOOH), schwertmannite ($Fe_8O_8(OH)_{4.5}(SO_4)_{1.75}$), and jarosite ($KFe_3(SO_4)_2(OH)_6$). Thermodynamic data from Ball and Nordstrom (1991) and Bigham et al. (1996).

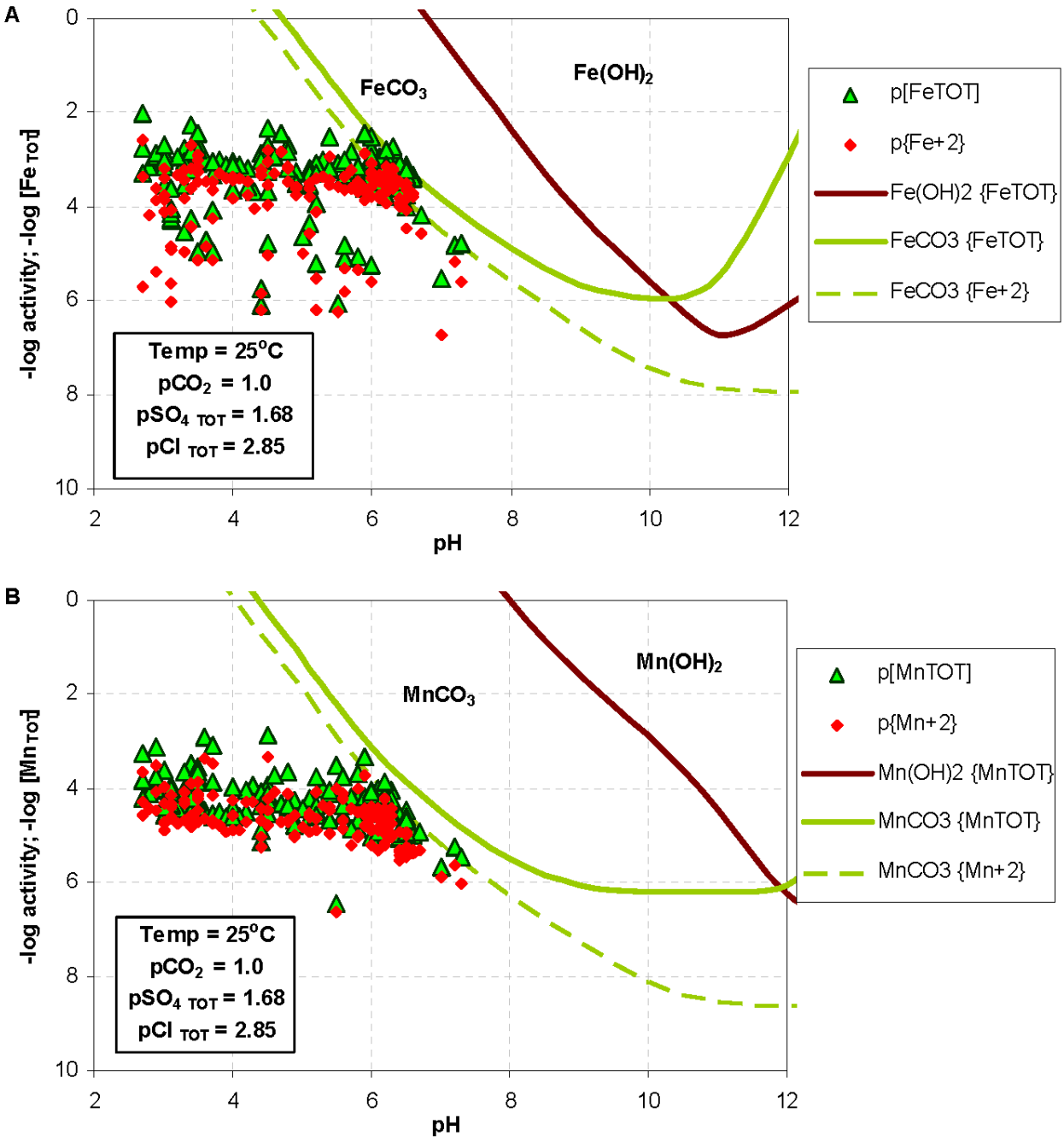

Figure 6. Ferrous iron and manganese solubility at 25 °C as a function of pH, pCO_2, pSO_4, and pCl: *A*, Total dissolved iron concentration and ferrous ion activity for 140 AMD samples and potential solubility control by $Fe(OH)_2$ and siderite ($FeCO_3$). *B*, Total dissolved manganese concentration and manganous ion activity for 140 AMD samples and potential solubility control by $Mn(OH)_2$ and rhodochrosite ($MnCO_3$). Thermodynamic data from Ball and Nordstrom (1991) and Stumm and Morgan (1996).

Total concentrations of Fe and activities of Fe^{+2} were undersaturated with respect to Fe(II) hydroxide, carbonate, and sulfate minerals at low to moderate pH (pH < 6) (Fig. 6A). However, the concentrations of Fe and activities of Fe^{+2} for near-neutral pH samples approached equilibrium with siderite ($FeCO_3$) (Fig. 6A). Most AMD samples with pH $\geq$ 6 had positive SI values for siderite, ranging as high as 0.9. In contrast, all the AMD samples were undersaturated with $Fe(OH)_2$ (Fig. 6A) and melanterite ($FeSO_4 \cdot 7H_2O$); SI for melanterite was -7.4 to -2.4 (Fig. 3H), indicating the Fe(II) hydroxide and sulfate phases can not precipitate from the AMD without increasing the pH or sulfate concentrations.

Dissolved manganese predominates as Mn^{II} species in AMD samples. As with Fe^{II}, the total concentration of Mn and activity of Mn^{+2} were undersaturated with respect to $Mn(OH)_2$, SO_4^{-2}, and CO_3^{-2} minerals at low to moderate pH (pH < 6) (Fig. 6B). At near-neutral pH, however, the concentration of Mn could be limited by equilibrium with a CO_3^{-2} phase such as rhodochrosite ($MnCO_3$) or impure siderite $(Fe,Mn)CO_3$ (Mozley, 1989). SI values for rhodochrosite and $MnSO_4$ ranged from -4.7 to -0.1 and -13.0 to -8.8, respectively (Fig. 3I). As previously indicated, many of these samples were saturated with siderite (Fig. 3H). Large increases in pH and decreases in Pco_2 would be necessary to precipitate $Mn(OH)_2$ instead of Mn(II)-bearing carbonates.

Calcite and aragonite ($CaCO_3$) commonly contain impurities that substitute for Ca, such as Mg, Mn^{+2}, Fe, Sr, Zn, Pb, and Ba (Hanshaw and Back, 1979). Siderite also commonly contains impurities such as Mg, Mn, and Zn (Mozley, 1989). Hence, dissolution of impure calcite, aragonite, and siderite can be a source of trace metals in AMD. Under oxidizing, acidic conditions, the carbonate minerals tend to dissolve, releasing the constituent Ba, Pb, and Zn as divalent cations. In contrast, at high pH, the cations can precipitate as SO_4^{-2}, CO_3^{-2} and/or OH^- minerals (Stumm and Morgan, 1996; Drever, 1997, p. 189-196). The cations also can be controlled by adsorption on iron oxides or aluminum oxides at near-neutral pH conditions (e.g. Winland et al., 1991; Kooner, 1993; Webster et al., 1998). Nevertheless, the relations between the concentrations of trace elements, pH, and/or SO_4^{-2} in CMD samples varied among the elements (Fig. 2), implying different origins or mechanisms could control their concentrations.

Figure 7A shows corresponding values of measured pH and Ca for the AMD samples relative to the theoretical solubility of calcite ($CaCO_3$) for Pco_2 of $10^{-3.5}$ atm (0.0316%) and $10^{-0.5}$ atm (31.6%) and the solubility of gypsum ($CaSO_4 \cdot 2H_2O$) for total dissolved SO_4^{-2} of 2,000 mg L^{-1}. Generally, the total concentrations of Ca in the AMD samples are less than or equal to equilibrium concentrations with gypsum or calcite (Fig. 7A). Corresponding SI values for calcite and gypsum ranged from -6.3 to 0.1 and -3.1 to -0.1, respectively (Fig. 3B and 3C), and were consistent with equilibrium boundaries based on the maximum Pco_2 and SO_4^{-2} concentrations of the AMD samples. These results indicate that the majority of AMD samples are undersaturated with calcite and gypsum. If the AMD encounters these minerals, the constituent elements and any impurities could be dissolved.

Concentrations of Ba generally were larger for anthracite discharges than bituminous discharges, and the concentrations increased with pH (Fig. 2), presumably because elevated SO_4^{-2} concentrations in the bituminous discharges or at low pH promoted the formation of insoluble barite ($BaSO_4$) (Fig. 7B). Computed SI values for barite ranged from -0.5 to 0.6, while those for witherite ($BaCO_3$) ranged from -9.6 to -3.7 (Fig. 3L). Hence, barite could be an

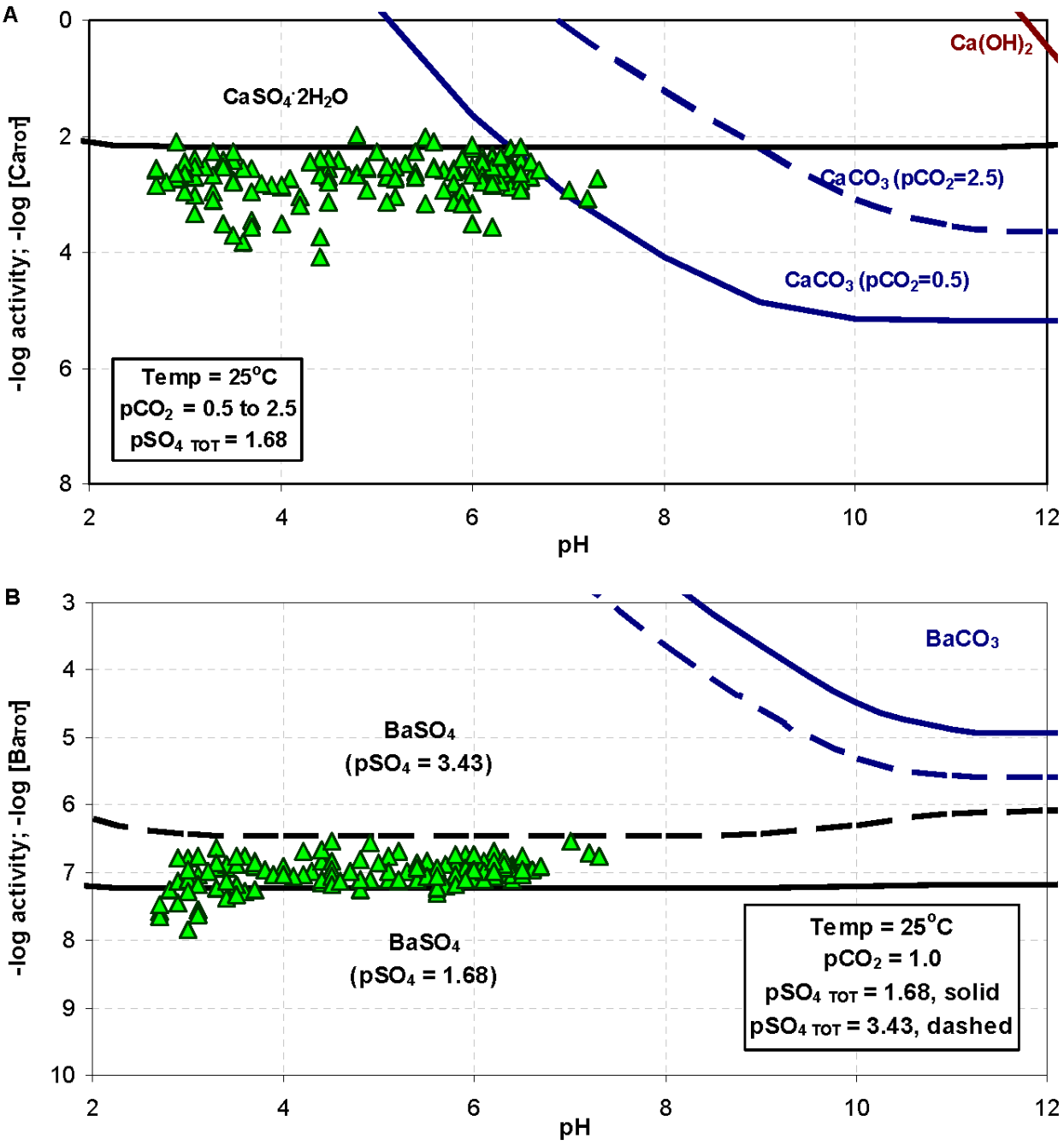

Figure 7. Calcium and barium solubility at 25 °C as a function of pH, pCO_2, pSO_4, and pCl: *A*, Total dissolved calcium for 140 AMD samples and potential solubility control by portlandite ($Ca(OH)_2$), calcite ($CaCO_3$), and gypsum ($CaSO_4 \cdot 2H_2O$). Calcite solubility for "open system" (constant $Pco_2 = 10^{-2.5}$ or $10^{-0.5}$ atm); gypsum solubility for sulfate = $10^{-1.68}$ M (2,000 mg L^{-1}). *B*, Total dissolved barium concentration for 140 AMD samples and potential solubility control by barite ($BaSO_4$) and witherite ($BaCO_3$).

important control on dissolved Ba concentrations. The barite solubility boundary in Fig. 7B will shift downward with increased SO_4^{-2} concentrations, whereas that for witherite will shift downward with increased Pco_2. Nevertheless, even for a 100 percent CO_2 atmosphere ($pCO_2 = 10^0$ atm) the witherite boundary will not overlap the AMD data. Although the median and maximum concentrations of Zn in bituminuous discharges exceeded those for anthracite discharges, the concentrations of Zn were comparable between anthracite and bituminous discharges at a particular pH; Zn concentrations decreased with increased pH (Figs. 2 and 8A). Generally, concentrations of zinc were undersaturated with all the zinc oxide, OH^-, SO_4^{-2}, CO_3^{-2}, or silicate minerals included in WATEQ4F (Ball and Nordstrom, 1991). Hence, the concentrations of dissolved Zn in AMD samples must be limited by other minerals or mechanisms.

Concentrations of lead, like Ba, were larger in anthracite discharges than bituminous discharges over the range of pH; however, in contrast with Ba, Pb concentrations decreased with increased pH (Figs. 2 and 8B). Lead concentrations in the AMD samples were substantially undersaturated with respect to likely secondary mineral phases, such as anglesite ($PbSO_4$) or cerrusite ($PbCO_3$). SI values for anglesite and cerrusite (Fig. 3K), and $Pb(OH)_2$ ranged from -5.3 to -2.5, -6.7 to -3.0, and -12.5 to -5.4, respectively. Hence, formation of these phases would not be feasible without increasing SO_4^{-2} or CO_3^{-2} concentrations or pH. The concentrations of dissolved lead in the AMD samples must be limited by other mechanisms. Coal and associated black shales are enriched sources of zinc and lead (Mason, 1966; Bragg et al., 1997); hence, it is unlikely that these metal concentrations are limited by the lack of supply. Zinc and Pb concentrations could be controlled by coprecipitation with barite and/or by adsorption on Fe oxides, schwertmannite, or another sulfate-bearing phase (e.g. Winland et al., 1991; Kooner, 1993; Coston et al., 1995; Webster et al., 1998). Although beyond the scope for this report, the geochemical model PHREEQC (Parkhurst and Appelo, 1999) may be useful to evaluate adsorption controls on the concentrations of trace metals in the AMD samples.

Summary and Conclusions

Water-quality data were collected in 1999 for 140 abandoned underground mines in bituminous and anthracite coal regions of Pennsylvania. The pH of ranged from 2.7 to 7.3, with the majority of samples having pH 2.5 to 4 (acidic) or pH 6 to 7.0 (near neutral). Generally bituminous discharges had smaller flow rates and were less mineralized than anthracite discharges with similar pH; flow rate increased with pH of the discharges. Increased pH with increased flow rate is consistent with dilution of initially acidic AMD with alkaline water. Dilution is more pronounced for anthracite discharges than bituminous discharges.

Bituminous discharges had higher median and maximum concentrations of alkalinity, acidity, SO_4^{-2}, Fe, Al, Mn, As, B, Co, Ni, Se, Y, and Zn than anthracite discharges, but lower median concentrations of dissolved Ba and Pb than anthracite discharges. Positive correlations between SO_4^{-2} and other constituents indicate similar origin, similar solubility-control mechanisms, and/or potential for ion-pairing.

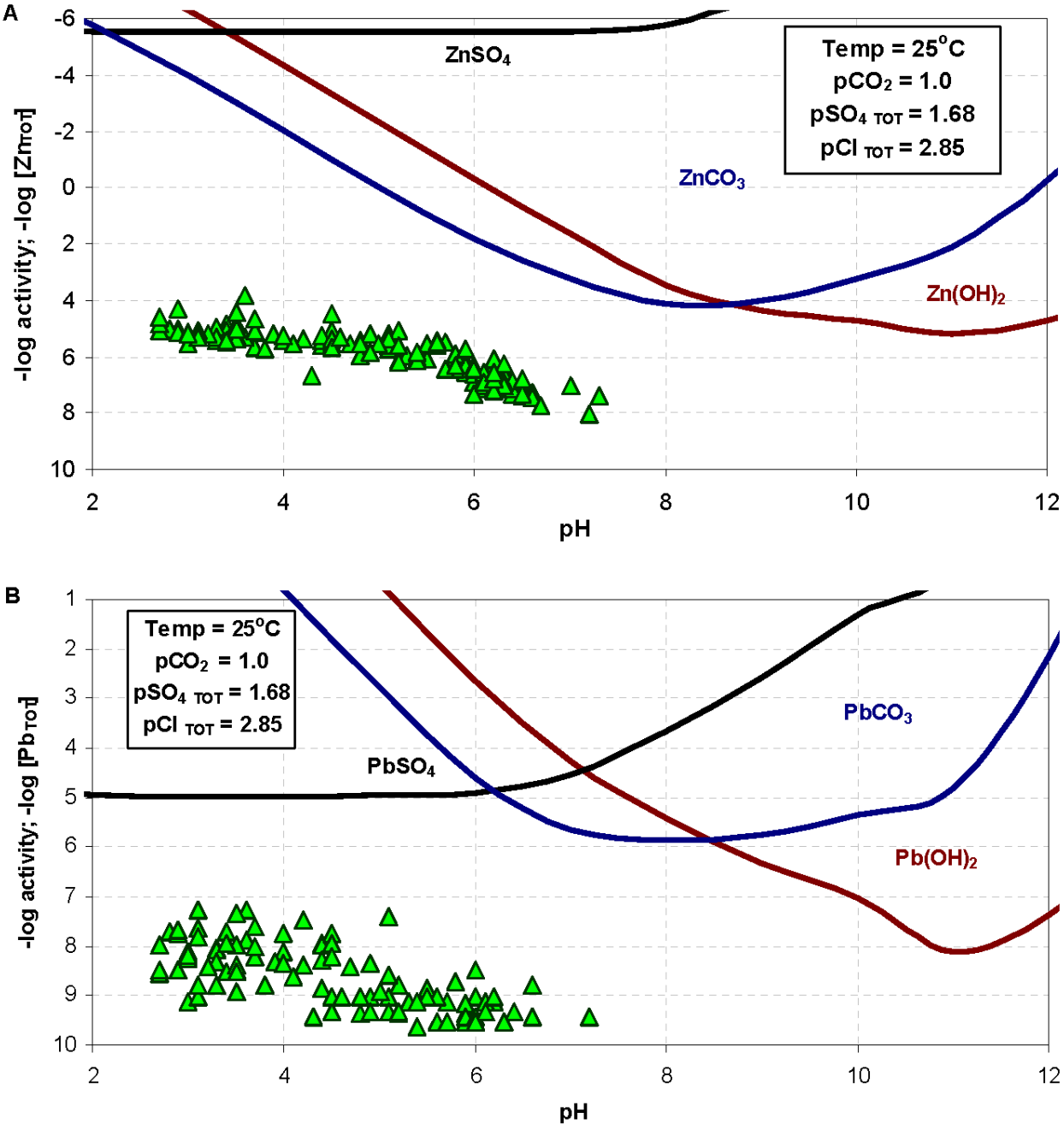

Figure 8. Zinc and lead solubility at 25 °C as a function of pH, pCO_2, pSO_4, and pCl: *A*, Total dissolved zinc for 140 AMD samples and potential solubility control by $Zn(OH)_2$, smithsonite ($ZnCO_3$), and zincite ($ZnSO_4$). *B*, Total dissolved lead concentration for 140 AMD samples and potential solubility control by anglesite ($PbSO_4$) and cerrusite ($PbCO_3$). Thermodynamic data from Ball and Nordstrom (1991).

Formation of $AlSO_4^+$ and $AlHSO_4^{+2}$ complexes adds to the total dissolved Al concentration at equilibrium with $Al(OH)_3$ or hydroxysulfate minerals and can account for 10 to 20 times greater concentrations of dissolved Al in bituminous discharges compared to anthracite discharges at similar pH. Similarly, the formation of $FeSO_4^+$ and $FeHSO_4^{+2}$ increases the solubility of Fe^{+3} in equilibrium with iron hydroxide or hydroxysulfate minerals.

Dissolved Al, Zn, and Pb concentrations and, to a lesser extent, SO_4^{-2} and Mn concentrations, were inversely correlated with pH; Fe concentrations were not correlated with pH; and Ba and alkalinity concentrations were positively correlated with pH. Inverse correlations between the pH and concentrations of Al and other metals could result from solubility control by OH^-, hydroxysulfate, and/or CO_3^{-2} minerals. Concentrations of Al and activities of Al^{+3} at pH $\geq$ 5.5 for the AMD samples were limited by equilibrium with amorphous to poorly crystalline $Al(OH)_3$, ($Al_2Si_2O_5(OH)_4$), allophane ($[Al(OH)_3]_{(1-x)}[SiO_2]_{(x)}$ where x = 1.24-0.135 pH), and/or kaolinite. Similarly, the activities of Fe^{+3} at pH $\geq$ 5.5 were controlled by equilibrium with $Fe(OH)_3$ or schwertmannite. Nevertheless, dissolved Fe and Mn in most samples were dominated by relatively soluble Fe^{+2} and Mn^{+2} species. At pH > 6, the precipitation of siderite ($FeCO_3$), rhodochrosite ($MnCO_3$), or impure siderite ($(Fe,Mn)CO_3$) could limit the maximum concentration of dissolved Fe and Mn.

Higher SO_4^{-2} concentrations but lower Pb and Ba concentrations in bituminous than anthracite discharges indicates increased SO_4^{-2} concentration limits the mobility of these metals. Most samples were saturated with barite ($BaSO_4$), but none were saturated with anglesite ($PbSO_4$). Lead potentially could be precipitated as an impurity with barite and/or controlled by adsorption to schwertmannite or another sulfate-bearing oxide.

High solubilities for various CO_3^{-2} minerals compared to dissolved Ca, Fe, Mn, Ba, Pb, and Zn, particularly at pH < 6, indicates the CO_3^{-2} minerals could be important sources of dissolved constituents in the mine drainage samples. However, additional qualitative and quantitative information on the composition and solubilities of impure CO_3^{-2} minerals would be needed to determine the actual sources and sinks of these elements.

Elevated concentrations of Ba and Pb in "dilute," greater volume anthracite discharges compared to "mineralized" bituminous discharges are noteworthy considering growing interest for developing water resources and extracting metals at abandoned mine sites. Although the anthracite water resource may contain acceptable concentrations of SO_4^{-2}e for industrial and domestic uses, the concentrations and mass loadings of Ba and Pb warrant consideration relative to the end use. Increasing concentrations of sulfate in solution may be beneficial for decreasing concentrations of Ba, Pb, and other potentially toxic constituents and could facilitate the recovery of elements such as Ba and Pb as SO_4^{-2} compounds at relatively low pH, while major ions such as Ca, Mg, Mn^{+2}, and Fe^{+2} ions remain in solution.

In conclusion, general relations among the pH, SO_4^{-2}, and dissolved metals described for underground mine discharges and the associated geochemical processes that control the water quality are applicable to the understanding of drainage from surface coal mines and metal mines. The same geochemical principles and tools also apply to chemical reactions associated with pH and pCO_2 changes and mineral precipitation during acidity titrations and treatment of mine drainage.

Acknowledgments

This work was conducted by the U.S. Geological Survey, in cooperation with the Southern Alleghenies Conservancy (SAC), and with support from the U.S. Environmental Protection Agency and the Pennsylvania Department of Environmental Protection. The author wishes to thank Donald R. Williams and Jeffrey B. Weitzel for their field and laboratory assistance, Robert Seal and Jane Hammarstrom for their analytical support, and Brandon Diehl and Brad Clemenson for their encouragement. The manuscript benefitted from reviews by Kevin J. Breen and Arthur W. Rose.

Literature Cited

Alpers, C. N., Nordstrom, D. K., and Ball, J. W., 1989, Solubility of jarosite solid solutions precipitated from acid mine waters, Iron Mountain, California, U.S.A.: Sciences Geologique, Bulletin, Strasbourg, v. 42, p. 281-298.

American Public Health Association, 1998a, Acidity (2310)/Titration method, In Clesceri, L. S., Greenberg, A. E., and Eaton, A. D. (eds), *Standard Methods for the Examination of Water and Wastewater* (20th): Washington, D.C., American Public Health Association, p. 2.24-2.26.

American Public Health Association, 1998b, Alkalinity (2320)/Titration method, In Clesceri, L. S., Greenberg, A. E., and Eaton, A. D. (eds), *Standard Methods for the Examination of Water and Wastewater* (20th): Washington, D.C., American Public Health Association, p. 2.26-2.29.

Baker, J. P., and Schofield, C. L., 1982, Aluminum toxicity to fish in acidic waters: Water Air Soil Pollution, v. 18, p. 289-309. http://dx.doi.org/10.1007/BF02419419.

Ball, J. W., and Nordstrom, D. K., 1991, User's manual for WATEQ4F with revised data base: U.S. Geological Survey Open-File Report 91-183, 189 p. (accessed on the Word Wide Web on July 13, 2004 at http://wwwbrr.cr.usgs.gov/projects/GWC_chemtherm/pubs/wq4fdoc.pdf)

Barnes, Ivan, and Clarke, F. E., 1969, Chemical properties of ground water and their corrosion and encrustation effects on wells: U.S. Geological Survey Professional Paper 498-D, p. D1-D58.

Berg, T. M., Barnes, J. H., Sevon, W. D., Skema, V. K., Wilshusen, J. P., and Yannaci, D. S., 1989, Physiographic provinces of Pennsylvania: Pennsylvania Geological Survey, 4th Series, Map 13, scale 1:2,000,000.

Berg, T. M., et al., 1980, Geologic map of Pennsylvania: Pennsylvania Geological Survey, Fourth Series, Map # 1, scale 1:2,500,000, 3 sheets.

Bigham, J. M., and Nordstrom, D. K., 2000, Iron and aluminum hydroxysulfate minerals from acid sulfate waters, In Jambor, J. L., Alpers, C. N., and Nordstrom, D. K., (eds.), *Sulfate minerals, crystallography, geochemistry and environmental significance*: Mineralogical Society of America Reviews in Mineralogy and Geochemistry, v. 40, p. 351-403.

Bigham, J. M., Schwertmann, U., Traina, S. J., Winland, R. L., and Wolf, M., 1996, Schwertmannite and the chemical modeling of iron in acid sulfate waters: Geochimica et Cosmochimica Acta, v. 60, p. 2111-2121. http://dx.doi.org/10.1016/0016-7037(96)00091-9.

Brady, K. B. C., Hornberger, R. J., and Fleeger, G., 1998, Influence of geology on post-mining water quality-Northern Appalachian Basin, In Brady, K. B. C., Smith, M. W., and Schueck, J. H., (eds.), *The prediction and prevention of acid drainage from surface coal mines in Pennsylvania*: Harrisburg, Pa., Pennsylvania Department of Environmental Protection, 5600-BK-DEP2256, p. 8.1-8.92.

Bragg, L. J., Oman, J. K., Tewalt, S. J., Oman, C. J., Rega, N. H., Washington, P. M., and Finkelman, R. B, 1997, U.S. Geological Survey Coal Quality (COALQUAL) Database, Version 2.0: U.S. Geological Survey Open-File Report 97-134.

Coston, J. A., Fuller, C. C. and Davis, J. A., 1995, Pb2+ and Zn2+ adsorption by a natural aluminum- and iron-bearing surface coating on an aquifer sand: Geochimica et Cosmochimica Acta, v. 59, p. 3535-3547. http://dx.doi.org/10.1016/0016-7037(95)00231-N.

Cravotta, C. A., III, 2004, Characteristics of abandoned mine drainage in Pennsylvania (abs.): Geological Society of America, Northeastern Section (39th Annual) and Southeastern Section (53rd Annual) Joint Meeting (March 25–27, 2004), GSA Abstracts with Programs Vol. 36, No. 2, March 2004.

Cravotta, C. A., III, and Kirby, C. S., 2004, Acidity and alkalinity in mine drainage--practical considerations, In *2004 National Meeting of the American Society of Mining and Reclamation and the 25th West Virginia Surface Mine Drainage Task Force, April 18-24, 2004*: American Society of Mining and Reclamation, p. 334-365.
https://doi.org/10.21000/JASMR04010334

Cravotta, C. A., III, Dugas, D. L., Brady, K. B. C., and Kovalchuk, T. E., 1994, Effects of selective handling of pyritic, acid-forming materials on the chemistry of pore gas and ground water at a reclaimed surface coal mine in Clarion County, PA, USA: U.S. Bureau of Mines Special Publication SP 06A, p. 365-374. Note page numbers are 366-374
https://doi.org/10.21000/JASMR04010366

Cravotta, C. A., III, Brady, K. B. C., Rose, A. W., and Douds, J. B., 1999, Frequency distribution of the pH of coal-mine drainage in Pennsylvania, In Morganwalp, D. W., and Buxton, H., (eds.), U.S. *Geological Survey Toxic Substances Hydrology Program--Proceedings of the technical meeting*: U.S. Geological Survey Water-Resources Investigations Report 99-4018A, p. 313-324.

Crock, J. G., Arbogast, B. F., and Lamothe, p. J., 1999, Laboratory methods for the analysis of environmental samples, In Plumlee G. S., and Logsdon, M. J., (eds.), *The Environmental Geochemistry of Mineral Deposits--Part A. Processes, techniques, and health issues*: Society of Economic Geologists, Reviews in Economic Geology, v. 6A, p. 265-287.

Drever, J. I., 1997, *The geochemistry of natural waters--Surface and groundwater environments* (3rd): Englewood Cliffs, N.J., Prentice-Hall, Inc., 436 p.

Edmunds, W. E., 1999, Bituminous coal, In Schultz, C. H., (ed.), *The geology of Pennsylvania*: Pennsylvania Geological Survey, 4th series, Special Publication 1, p. 470-481.

Eggleston, J. R., Kehn, T. M., and Wood, G. H., Jr., 1999, Anthracite, In Schultz, C. H., (ed.), *The geology of Pennsylvania*: Pennsylvania Geological Survey, 4th series, Special Publication 1, p. 458-469.

Elder, J. F., 1988, Metal biogeochemistry in surface-water systems--a review of principles and concepts: U.S. Geological Survey Circular 1013, 43 p.

Ficklin, W. H., and Mosier, E. L., 1999, Field methods for sampling and analysis of environmental samples for unstable and selected stable constituents, In Plumlee G.S., and Logsdon, M.J., (eds.), *The Environmental Geochemistry of Mineral Deposits--Part A. Processes, techniques, and health issues*: Society of Economic Geologists, Reviews in Economic Geology, v. 6A, p. 249-264.

Fishman, M. J., and Friedman, L. C., (eds.), 1989, Methods for determination of inorganic substances in water and fluvial sediments: U.S. Geological Survey Techniques of Water-Resources Investigations, Book 5, Chapter A1, 545 p.

Growitz, D. J., Reed, L. A., and Beard, M. M., 1985, Reconnaissance of mine drainage in the coal fields of eastern Pennsylvanian: U.S. Geological Survey Water Resources Investigations Report 83-4274, 54 p.

Hanshaw, B. B., and Back, William, 1979, Major geochemical processes in the evolution of carbonate-aquifer systems: Journal of Hydrology, v. 43, p. 287-312. http://dx.doi.org/10.1016/0022-1694(79)90177-X.

Houben, G., 2003, Iron oxide incrustations in wells, Part 1—Genesis, mineralogy and geochemistry: Applied Geochemistry, v. 18, p. 927-939. http://dx.doi.org/10.1016/S0883-2927(02)00242-1.

Hyman, D. M., and Watzlaf, G. R., 1997, Metals and other components of coal mine drainage as related to aquatic life standards, In *Proceedings of the 1997 National Meeting of the American Society for Surface Mining and Reclamation, May 10-15, 1997, Austin, Texas*: American Society for Surface Mining and Reclamation, p. 531-545.
https://doi.org/10.21000/JASMR97010531

Kirby, C. S., and Cravotta, C. A., III, 2005a, Net alkalinity and net acidity 1: Theoretical considerations: Applied Geochemistry, v. 20, p. 1920-1940. http://dx.doi.org/10.1016/j.apgeochem.2005.07.002.

Kirby, C. S., and Cravotta, C. A., III, 2005b, Net alkalinity and net acidity 2: Practical considerations: Applied Geochemistry, v. 20, p. 1941-1964.

http://dx.doi.org/10.1016/j.apgeochem.2005.07.003.

Kooner, Z. S., 1993, Comparative study of adsorption behavior of copper, lead, and zinc onto goethite in aqueous systems: Environmental Geology, v. 21, p. 342-250. http://dx.doi.org/10.1007/BF00775914.

Langmuir, Donald, 1997, *Aqueous environmental geochemistry*: New Jersey, Prentice-Hall.

Mason, B., 1966, Principles of Geochemistry: New York , John Wiley & Sons.

Miller, S. D., 1980, Sulfur and hydrogen ion buffering in pyritic strip mine spoil, In Trudinger, p. A., and Walter, M. R., (eds.), *Biogeochemistry of ancient and modern environments*: New York, Springer-Verlag, p. 537-543.

Mozley, P. S., 1989, Relationship between depositional environment and the elemental composition of early diagenetic siderite: Geology, v. 17, p. 704-706. http://dx.doi.org/10.1130/0091-7613(1989)017<0704:RBDEAT>2.3.CO;2.

Nordstrom, D. K., 1977, Thermochemical redox equilibria of ZoBell's solution: Geochimica et Cosmochimica Acta, v. 41, p. 1835-1841. http://dx.doi.org/10.1016/0016-7037(77)90215-0.

Nordstrom, D. K., 2000, Advances in the hydrochemistry and microbiology of acid mine waters: International Geology Review, v. 42, p. 499-515. http://dx.doi.org/10.1080/00206810009465095.

Nordstrom, D. K., 2004, Modeling Low-temperature Geochemical Processes, In Drever, J. I., (ed.), *Surface and Ground Water, Weathering, and Soils*: Elsevier, Treatise on Geochemistry, v. 5., p. 37-72.

Nordstrom, D. K., and Alpers, C. N., 1999, Geochemistry of acid mine waters, In Plumlee, G. S., and Logsdon, M. J., (eds.), *The Environmental Geochemistry of Mineral Deposits--Part A. Processes, methods, and health issues*: Reviews in Economic Geology, v. 6A, p. 133-160.

Nordstrom, D. K., and Ball, J. W., 1986, The geochemical behavior of aluminum in acidified surface waters: Science, v. 232, p. 54-58. http://dx.doi.org/10.1126/science.232.4746.54.

Nordstrom, D. K., Alpers, C. N., Ptacek, C. J., and Blowes, D. W., 2000, Negative pH and extremely acidic mine waters from Iron Mountain, California: Environmental Science & Technology, v. 34, p. 254-258. http://dx.doi.org/10.1021/es990646v.

Nordstrom, D. K., Jenne, E. A., and Ball, J. W., 1979, Redox equilibria of iron in acid mine waters, In Jenne, E. A., (ed.), *Chemical modeling in aqueous systems--Speciation, sorption, solubility, and kinetics*: American Chemical Society Symposium Series 93, p. 51-79.

Northern and Central Appalachian Basin Coal Regions Assessment Team, 2000, 2000 resource assessment of selected coal beds and zones in the northern and central Appalachian Basin coal regions: U.S. Geological Survey Professional Paper 1625C, CD-ROM, version 1.0.

Parkhurst, D. L., and Appelo, C. A. J., 1999, User's guide to PHREEQC (Version 2)--A computer program for speciation, batch-reaction, one-dimensional transport, and inverse geochemical calculations: U.S. Geological Survey Water-Resources Investigations Report 99-4259, 312 p.

Pennsylvania Department of Environmental Protection, 2002, 2002 Pennsylvania water quality assessment 305(b) report: Harrisburg, Pa., Pennsylvania Department of Environmental Protection, 3800-BK-DEP2530 5/2/2002, 61 p.

Rantz, S. E., and others, 1982a, Measurement and computation of streamflow--1. Measurement of stage and discharge: U.S. Geological Survey Water-Supply Paper 2175, 284 p.

Rantz, S. E., and others, 1982b, Measurement and computation of streamflow--2. Computation of discharge: U.S. Geological Survey Water-Supply Paper 2175, 631 p.

Robbins, E. I., Nord, G. L., Savela, C. E., Eddy, J. I., Livi, K. J. T., Gullett, C. D., Nordstrom, D. K., Chou, I. -M., and Briggs, K. M., 1996, Microbial and mineralogical analysis of aluminum-rich precipitates that occlude porosity in a failed anoxic limestone drain, Monongalia County, West Virginia, In Chiang, Shiao-Hung (ed.), Coal-energy and the environment: Pittsburgh, Pa., Reed & Witting Company, Proceedings Thirteenth Annual International Pittsburgh Coal Conference, v. 2, p. 761-767.

Robbins, E. I., Cravotta, C. A., III, Savela, C. E., and Nord, G. L., Jr., 1999, Hydrobiogeochemical interactions in "anoxic" limestone drains for neutralization of acidic mine drainage: Fuel, v. 78, p. 259-270. http://dx.doi.org/10.1016/S0016-2361(98)00147-1.

Rose, A. W., and Cravotta, C. A., III, 1998, Geochemistry of coal-mine drainage, In Brady, K. B. C., Smith, M. W., and Schueck., J., (eds.), *Coal Mine Drainage Prediction and Pollution Prevention in Pennsylvania*: Harrisburg, Pa., Pennsylvania Department of Environmental Protection, 5600-BK-DEP2256, p. 1.1-1.22

Rose, A. W., Hawkes, H. E., and Webb, J. S., 1979, *Geochemistry in mineral exploration*: New York, Academic Press, 657 p.

Smith, K. S., and Huyck, H. L. O., 1999, An overview of the abundance, relative mobility, bioavailability, and human toxicity of metals, In Plumlee, G. S., and Logsdon, M. J., (eds.), *The Environmental Geochemistry of Mineral Deposits--Part A. Processes, methods, and health issues*: Reviews in Economic Geology, v. 6A, p. 29-70.

Southern Alleghenies Conservancy, 1998, Findings for the inventory and monitoring phase of the resource recovery program: Bedford, Pa., Southern Alleghenies Conservancy, unpublished report, 74 p.

Stumm, Werner, and Morgan, J. J., 1996, *Aquatic chemistry--Chemical equilibria and rates in natural waters* (3rd): New York, John Wiley and Sons, 1022 p.

Thomas, R. C. and Romanek, C. S., 2002, Passive treatment of low-pH, ferric dominated acid rock drainage in a vertical flow wetland--II. Metal removal, In P*roceedings of the 19th Annual Meeting of American Society of Mining and Reclamation, Lexington, Kentucky, June 9-13, 2002*: American Society of Mining and Reclamation, p. 752-775.
https://doi.org/10.21000/JASMR02010752

U.S. Environmental Protection Agency, 2000, Drinking water standards and health advisories (summer 2000): U.S. Environmental Protection Agency, 12 p. (http://www.epa.gov/OST).

U.S. Environmental Protection Agency, 2002a, National primary drinking water standards: U.S. Environmental Protection Agency EPA/816-F-02-013, July 2002, 7 p. (http://www.epa.gov/safewater).

U.S. Environmental Protection Agency, 2002b, National recommended water quality criteria--2002: U.S. Environmental Protection Agency EPA/822-R-02-047, 33 p.

U.S. Geological Survey, variously dated, National field manual for the collection of water-quality data: U.S. Geological Survey Techniques of Water-Resources Investigations, book 9, chaps. A1-A9, variously paged (http://pubs. water. usgs. gov/twri9A).

Webster, J. G., Swedlund, P. J. and Webster, K. S., 1998, Trace metal adsorption onto an acid mine drainage iron(III) oxy hydroxy sulfate: Environmental Science & Technology, v. 32, p. 1361-1368.
http://dx.doi.org/10.1021/es9704390.

Whittemore, D.O., and Langmuir, Donald, 1975, The solubility of ferric oxyhydroxides in natural waters: Ground Water, v. 13, p. 360-365. http://dx.doi.org/10.1111/j.1745-6584.1975.tb03600.x.

Williams, D. J., Bigham, J. M., Cravotta, C. A., III, Traina, S. J., Anderson, J. E., and Lyon, G., 2002, Assessing mine drainage pH from the color and spectral reflectance of chemical precipitates: Applied Geochemistry, v. 17, p. 1273-1286. http://dx.doi.org/10.1016/S0883-2927(02)00019-7

Winland, R. L., Traina, S. J., and Bigham, J. M., 1991, Chemical composition of ochreous precipitates from Ohio coal mine drainage: Journal of Environmental Quality, v. 20, p. 452-460. http://dx.doi.org/10.2134/jeq1991.00472425002000020019x.

Wood, C. R., 1996, Water quality of large discharges from mines in the anthracite region of eastern Pennsylvania: U.S. Geological Survey Water-Resources Investigations Report 95-4243, 68 p.

Wood, G. H., Jr., Kehn, T. M., and Eggleston, J. R., 1986, Deposition and structural history of the Pennsylvania Anthracite region, In Lyons, P. C., and Rice, C. L., (Eds.), Paleoenvironmental and tectonic controls in coal-forming basins of the United States: Geological Society of America Special Paper 210, p. 31-47. http://dx.doi.org/10.1130/SPE210-p31.

Wood, W. W., 1976, Guidelines for the collection and field analysis of ground-water samples for selected unstable constituents: U.S. Geological Survey Techniques of Water Resources Investigations, Book 1, Chapter D2, 24 p.

Yu, J. -Y., Heo, B., Choi, I. -K., Cho, J. -P., and Change, H. -W., 1999, Apparent solubilities of schwertmannite and ferrihydrite in natural stream waters polluted by mine drainage: Geochimica et Cosmochimica Acta, v. 63, p. 3407-3416. http://dx.doi.org/10.1016/S0016-7037(99)00261-6.

Table A1. Thermodynamic equilibrium constants at 25 °C used in constructing stability diagrams with species involving aqueous carbonate and sulfate complexes[a] [pK = -log(K), where K is equilibrium constant at 25 °C]

Carbonate Species			Sulfate Species	
$pKco_2$	pK_{1CO3}	pK_{2CO3}	pK_{1SO4}	pK_{2SO4}
1.47	6.35	10.33	-3.00	1.99

a. Thermodynamic data from Ball and Nordstrom (1991) for equations below, where A=CO_3 or SO_4, square brackets denote concentration, pointed brackets denote activity, and Pco_2 is partial pressure of CO_2 in atmospheres:
$H_2A = HA^- + H^+$; $HA^- = A^{-2} + H^+$; $[A_{TOT}] = [H_2A] + [HA^-] + [A^{-2}]$; $K_{1A} = \{HA^-\}\{H^+\} / \{H^2A\}$; $K_{2A} = \{A^{-2}\}\{H^+\} / \{HA^-\}$.
$p\{H_2CO_3^*\} = Pco_2 + pKco_2$; $p\{HCO_3^-\} = p\{H_2CO_3^*\} + pK_{1CO3} - pH$; $p\{CO_3^{-2}\} = p\{H_2CO_3^*\} + pK_{1CO3} + pK_{2CO3} - 2pH$;
$p\{H_2SO_4\} = p([SO_{4\,TOT}] / (1 + K_{1SO4}/\{H^+\} + K_{1SO4}K_{2SO4}/\{H^+\}^2))$; $p\{HSO_4^-\} = p\{H_2SO_4\} + pK_{1SO4} - pH$; $p\{SO_4^{-2}\} = p\{H_2SO_4\} + pK_{1SO4} + pK_{2SO4} - 2pH$.

Table A2. Thermodynamic equilibrium constants at 25 °C used in constructing stability diagrams for mononuclear metal compounds and aqueous complexes[a] [pK = -log(K) or -log(*B), where K and *B are equilibrium constants at 25 °C; n.a., not applicable]

Cation	Hydroxide Minerals[b]		Sulfate Minerals		Carbonate Minerals		Hydroxyl Species[c]				Chloride Species				Sulfate Species[d]			Carbonate Species[d]		
	pK^*a	pK^*c	pKa_{MSO4}	pKc_{MSO4}	pKa_{MCO3}	pKc_{MCO3}	p^*B_1	p^*B_2	p^*B_3	p^*B_4	pK_{1Cl}	pK_{2Cl}	pK_{3Cl}	pK_{4Cl}	pK_{1SO4}	pK_{2SO4}	pK_{HSO4}	pK_{1CO3}	pK_{2CO3}	pK_{HCO3}
Al^{3+}	-10.8	-8.11	3.23	-22.7	n.a.	n.a.	5.0	10.1	16.9	22.7	n.a.	n.a.	n.a.	n.a.	-3.02	-4.92	-0.46	n.a.	n.a.	n.a.
Ba^{2+}	n.a.	n.a.	9.97	n.a.	8.56	n.a.	13.47	n.a.	n.a.	n.a.	n.a.	n.a.	n.a.	n.a.	-2.70	n.a.	n.a.	-2.71	n.a.	-0.98
Ca^{2+}	-22.8	n.a.	4.36	4.58	8.34	8.48	12.78	n.a.	n.a.	n.a.	n.a.	n.a.	n.a.	n.a.	-2.30	n.a.	n.a.	-3.22	n.a.	-1.11
Fe^{2+}	12.9	n.a.	2.21	n.a.	10.45	10.89	9.50	20.57	31.00	n.a.	-0.14	n.a.	n.a.	n.a.	-2.25	n.a.	-1.08	-4.38	n.a.	-2.0
Fe^{3+}	4.30	1.40	n.a.	n.a.	n.a.	n.a.	2.19	5.67	12.56	21.6	-1.48	-2.13	-1.13	n.a.	-4.04	-5.38	-2.48	n.a.	n.a.	n.a.
Mn^{2+}	-15.2	n.a.	-2.67	n.a.	10.39	11.13	10.59	22.20	34.80	n.a.	-0.61	-0.25	0.31	n.a.	-2.25	n.a.	n.a.	-4.90	n.a.	-1.95
Pb^{2+}	-8.15	n.a.	7.79	n.a.	13.13	n.a.	7.71	17.12	28.06	39.7	-1.60	-1.80	-1.70	-1.38	-2.75	-3.47	n.a.	-7.24	-10.64	-2.9
Zn^{2+}	11.5	12.45	1.96	-3.01	10	n.a.	8.96	16.9	28.4	41.2	-0.43	-0.45	-0.50	-0.20	-2.37	-3.28	n.a.	-5.3	-9.63	-2.1

a. Thermodynamic data from Ball and Nordstrom (1991), Stumm and Morgan (1996), and Bigham et al. (1996).

b. Hydroxide mineral: pK* for $M(OH)_z + zH^+ = M^{z+} + zH_2O$ where z indicates charge on uncomplexed cation. Denoted with "a" for more soluble, amorphous phase and "c" for less soluble, crystalline phase.

c. For the general association reaction where "n" protonated ligands are added to "m" metal ions, speciation can be described as: $mM^{+z} + nHL = ML_n^{(z-n)} + nH^+$. For hydrolysis reactions, $L = OH^-$, and $HL = H_2O$. The overall equilibrium constant for this reaction can be written: $*B_n = \{M_mL_n^{(z-n)}\}\{H^+\}^n / \{M^{+z}\}^m\{HL\}^n$, where brackets denote activity of aqueous species. Rewriting and expressing as logarithm: $Log*B_n = Log\{M_mL_n^{(z-n)}\} - mLog\{M^{+z}\} - nLog\{HL\} - n(pH)$. See example computations for lead in Table A2.

Table A3. Equilibrium reactions and corresponding mass-balance equations used to compute stabilities of aqueous lead species and solid lead compounds [pK = -log(K) or -log(*B), where K and *B are equilibrium constants at 25 °C]

Equilibrium Reaction	Equilibrium Constant Equation	pK[a]	Expression for –Log Activity of Aqueous Complex
$Pb(OH)_2$ (s) + 2 H^+ = Pb^{+2} + 2 H_2O	$K_{Hydroxide} = \{Pb^{+2}\}/\{H^+\}^2$	-8.15	$p\{Pb^{+2}\} = pK_{Hydroxide} + 2\ pH$
$PbSO_4$ (s) = Pb^{+2} + SO_4^{-2}	$K_{Anglesite} = \{Pb^{+2}\}\{SO_4^{-2}\}$	7.79	$p\{Pb^{+2}\} = pK_{Anglesite} - p\{SO_4^{-2}\}$
$PbCO_3$ (s) = Pb^{+2} + CO_3^{-2}	$K_{Cerrusite} = \{Pb^{+2}\}\{CO_3^{-2}\}$	13.13	$p\{Pb^{+2}\} = pK_{Cerrusite} - p\{CO_3^{-2}\}$
Pb^{+2} + H_2O = $Pb(OH)^+$ + H^+	$*B_1 = \{Pb(OH)^+\}\{H^+\}/\{Pb^{+2}\}$	7.71	$p\{Pb(OH)^+\} = p*B_1 + p\{Pb^{+2}\} - pH$
Pb^{+2} + 2 H_2O = $Pb(OH)_2^0$ + 2 H^+	$*B_2 = \{Pb(OH)_2^0\}\{H^+\}^2/\{Pb^{+2}\}$	17.12	$p\{Pb(OH)_2^0\} = p*B_2 + p\{Pb^{+2}\} - 2\ pH$
Pb^{+2} + 3 H_2O = $Pb(OH)_3^-$ + 3 H^+	$*B_3 = \{Pb(OH)_3^-\}\{H^+\}^3/\{Pb^{+2}\}$	28.06	$p\{Pb(OH)_3^-\} = p*B_3 + p\{Pb^{+2}\} - 3\ pH$
Pb^{+2} + 4 H_2O = $Pb(OH)_4^{-2}$ + 4 H^+	$*B_4 = \{Pb(OH)_4^{-2}\}\{H^+\}^4/\{Pb^{+2}\}$	39.70	$p\{Pb(OH)_4^{-2}\} = p*B_4 + p\{Pb^{+2}\} - 4\ pH$
Pb^{+2} + Cl^- = $PbCl^+$	$K_{1Cl} = \{PbCl^+\}/(\{Pb^{+2}\}\{Cl^-\})$	-1.60	$p\{PbCl^+\} = pK_{1Cl} + p\{Pb^{+2}\} + p\{Cl^-\}$
Pb^{+2} + 2 Cl^- = $Pb(Cl)_2^0$	$K_{2Cl} = \{Pb(Cl)_2^0\}/(\{Pb^{+2}\}\{Cl^-\}^2)$	-1.80	$p\{Pb(Cl)_2^0\} = pK_{2Cl} + p\{Pb^{+2}\} + 2\ p\{Cl^-\}$
Pb^{+2} + 3 Cl^- = $Pb(Cl)_3^-$	$K_{3Cl} = \{Pb(Cl)_3^-\}/(\{Pb^{+2}\}\{Cl^-\}^3)$	-1.70	$p\{Pb(Cl)_3^-\} = pK_{3Cl} + p\{Pb^{+2}\} + 3\ p\{Cl^-\}$
Pb^{+2} + 4 Cl^- = $Pb(Cl)_4^{-2}$	$K_{4Cl} = \{Pb(Cl)_4^{-2}\}/(\{Pb^{+2}\}\{Cl^-\}^4)$	-1.38	$p\{Pb(Cl)_4^{-2}\} = pK_{4Cl} + p\{Pb^{+2}\} + 4\ p\{Cl^-\}$
Pb^{+2} + SO_4^{-2} = $PbSO_4^0$	$K_{1SO4} = \{PbSO_4^0\}/(\{Pb^{+2}\}\{SO4^{-2}\})$	-2.75	$p\{PbSO_4^0\} = pK_{1SO4} + p\{Pb^{+2}\} + p\{SO_4^{-2}\}$
Pb^{+2} + 2 SO_4^{-2} = $Pb(SO_4)_2^{-2}$	$K_{2SO4} = \{Pb(SO_4)_2^{-2}\}/(\{Pb^{+2}\}\{SO_4^{-2}\}^2)$	-3.47	$p\{Pb(SO_4)_2^{-2}\} = pK_{2SO4} + p\{Pb^{+2}\} + 2\ p\{SO_4^{-2}\}$
Pb^{+2} + HCO_3^- = $PbHCO_3^+$	$K_{HCO3} = \{PbHCO_3^+\}/(\{Pb^{+2}\}\{HCO_3^-\})$	-2.90	$p\{PbHCO_3^+\} = pK_{HCO3} + p\{Pb^{+2}\} + p\{HCO_3^-\}$
Pb^{+2} + CO_3^{-2} = $PbCO_3^0$	$K_{1CO3} = \{PbCO_3^0\}/(\{Pb^{+2}\}\{CO3^{-2}\})$	-7.24	$p\{PbCO_3^0\} = pK_{1CO3} + p\{Pb^{+2}\} + p\{CO_3^{-2}\}$
Pb^{+2} + 2 CO_3^{-2} = $Pb(CO_3)_2^{-2}$	$K_{2CO3} = \{Pb(CO_3)_2^{-2}\}/(\{Pb^{+2}\}\{CO_3^{-2}\}^2)$	-10.64	$p\{Pb(CO_3)_2^{-2}\} = pK_{2CO3} + p\{Pb^{+2}\} + 2\ p\{CO_3^{-2}\}$

Mass-Balance Expression[b]

$$[Pb_{TOT}] = [Pb^{+2}]+[Pb(OH)^+]+[Pb(OH)_2^0]+[Pb(OH)_3^-]+[Pb(OH)_4^{-2}]+[PbCl^-]+[PbCl_2^0]+[PbCl_3^-]+[PbCl_4^{-2}]+[PbSO_4^0]+[Pb(SO_4)_2^{-2}]+[PbHCO_3^+]+[PbCO_3^0]+[Pb(CO_3)_2^{-2}]$$

$$[Pb_{TOT}] = \{Pb^{+2}\}\ (1 + *B_1\{H^+\}^{-1} + *B_2\{H^+\}^{-2} + *B_3\{H^+\}^{-3} + *B_4\{H^+\}^{-4} + K_{1Cl}\{Cl^-\} + K_{2Cl}\{Cl^-\}^2 + K_{3Cl}\{Cl^-\}^3 + K_{4Cl}\{Cl^-\}^4 + K_{1SO4}\{SO_4^{-2}\} + K_{2SO4}\{SO_4^{-2}\}^2 + K_{HCO3}\{HCO_3^-\} + K_{1CO3}\{CO_3^{-2}\} + K_{2CO3}\{CO_3^{-2}\}^2)$$

a. Thermodynamic data from Ball and Nordstrom (1991).

b. Square brackets denote concentration; pointed brackets denote activity. Total concentration equals sum of concentrations of individual species, computed neglecting activity coefficients (e.g. Drever, 1997, p. 200-203; Langmuir, 1997, p. 248-255). Precise estimate of concentration requires division of the activity of each aqueous specie by its activity coefficient.